HAYATI
Journal of Biosciences

Vol. 30 No. 1, January 2023 113-121
DOI:10.4308/hjb.30.1.113-121
ISSN: 1978-3019
EISSN: 2086-4094

In Silico Study of Anticancer Activity of Red Betel Leaves Bioactive Compounds against Colon Cancer Marker Proteins

Mutmainnah Agustiawan Umar[1], Mega Safithri[1,2*], Rahadian Pratama[1]

[1]*Department of Biochemistry, Faculty of Mathematic and Natural Sciences, Bogor Agricultural University, Dramaga Campus, Bogor, Indonesia*
[2]*Tropical Biopharmaca Research Center (Biopharmaca), Institute for Research and Community Service, IPB University, Bogor, Indonesia*

ARTICLE INFO

Article history:
Received June 13, 2022
Received in revised form August 11, 2022
Accepted August 15, 2022

KEYWORDS:
Colorectal,
Docking,
Ligands,
Molecular,
Receptors

ABSTRACT

Colon cancer or colorectal cancer is one of the major health problems in the world. Previous research has proven that red betel leaves extract has anticancer activity against breast cancer cells. The study aimed to look at the potential of compounds contained in red betel ethyl acetate fraction as anticancer substances for colon cancer by conducting in silico tests through the docking of three colon cancer biomarker receptors against eight red betel leaves compounds. The parameters of binding affinity energy and inhibition constant used in the molecular docking analysis showed that there are several compounds that have the potential as inhibitors against colon cancer marker proteins to inhibit the development of colorectal cancer and have high bioavalibility as oral drugs. Based on *in silico* test it is known that the compound N-1,N-9-Bis [E-(2-nitophenyl) methylene] non anedihydrazide has the highest inhibition of human leukotriene A4 hydrolase receptor with binding affinity energy of 11.3160 Kcal/mol. The next compound is 4-({4,6-Bis[3R,5S)-3,5-diamino-1-piperydinyl]-1,3,5-traizin-2-yl}amino) benzenosulfon amide which has the highest inhibition in Chek1 with binding affinity energy of 9.7110 Kcal/mol, and the compound 4-(4-methoxy-phenylamino)-2,3-dihydro-1H-4a, 9-diaza-cyclopenta (b) fluorine-10-carbonitrile has the highest inhibition in the Bcl 2 navitoclax analog receptor with binding affinity energy of 8.4470 Kcal/mol.

1. Introduction

Colon or colorectal cancer is a malignant tumor that arises from the epithelial tissue of the colon or rectum. There are several treatments that can be done to treat colorectal cancer, including surgery, radiotherapy, and adjuvant chemotherapy (Sayuti and Nouva 2019). Some chemotherapy drugs that have been discovered today have a mechanism of action by inducing cytotoxicity, some of which are by influencing DNA replication transcription, activation of death receptor signals, as well as by activation of mitochondrial pathways. Those mechanisms can cause apoptosis of cancer cells and prevent metastases. However, chemotherapy drugs also have side effects, one of which is that it can interfere with body performance such as renal toxicity or cartilage suppression (Florea and Busselber 2011). The side effects caused by chemotherapy encourage researchers to develop herbal medicine that can replace the role of synthetic chemotherapy drugs that are relatively more effective in increasing the immunity of patients with cancer (Rizki *et al.* 2015).

One of the plants that has the potential to be efficacious in reducing the malignant effects of colon cancer is red betel. This is because the water extract of red betel leaves contains phytochemical compounds in the form of flavonoids, tannins, and alkaloids (Safithri *et al.* 2016). Ethyl acetate which is a semipolar solvent is able to attract compounds with a wide polarity range from polar to nonpolar, so that it is able to attract such compounds (Putri *et al.* 2013). The use of active compounds from fraction with ethyl acetate solvent is expected to obtain high antioxidant activity. Several studies have proven that semipolar solvent such as ethyl acetate have a stronger ability as an antidote to free radicals than methanol, ethanol, chloroform, petroleum ether, and hexane solvent (Suryanto and Momuat 2017).

* Corresponding Author
E-mail Address: safithri@apps.ipb.ac.id

In addition, the *in vitro* method shows that red betel water extract has the potential to be an activator of the SOD enzyme with the highest SOD activity of 3.41 U/ml (Safithri 2012).

Related to anticancer research, also the results of the *in vitro* study related to cancer, methanol extract of red betel leaves can inhibit the growth of breast cancer (T47D) through inhibition of phosphorylation p44/p42, which is a protein tyrosine kinase that plays a very important role in regulating the growth, differentiation, and survival of a cell (Wicaksono *et al.* 2009). Further study using the *in vivo* method based on the Brine Shrimp Lethality Test (BSLT) showed that the greater the concentration of red betel methanol extract, the greater the mortality of Artemia salina. The extract is said to be active or has anticancer activity according to the BSLT method if it has LC_{50}<1,000 µg ml^{-1}, the results obtained in this study have an average value of 70,013 µg ml^{-1}, so it is concluded that the methanol extract of red betel leaves has anticancer activity (Rosyadi *et al.* 2020).

Based on the previous research about the potentials of red betel leaves, it is necessary to conduct research related to its potential as a colon anticancer by *in silico* method. This study aims to see the potential of compounds contained in red betel ethyl acetate fraction which has the potential to be an anticancer for colon cancer with *in silico* test through the docking of three receptors of colonic cancer biomarkers against compounds of the ethyl acetate fraction of red betel leaves.

2. Materials and Methods

2.1. Protein Structure Quality Analysis

Analysis of the structure quality of each receptor, consisting of Human Leukotriene A4 hydrolase, Chek1, and Bcl 2 navitoclax analog was carried out on the PROCHECK website (https://servicesn.mbi.ucla.edu/PROCHECK/). The receptors structures from modeling results that have been downloaded in PDB format were previously uploaded on the website. In the next stage, the quality of the structure from modeling result was analyzed to identify stable amino acid residues, where these residues were divided into four quadrants. The four quadrants include most favoured regions, additional allowed regions, generously allowed regions, and disallowed regions (Kurnia and Ruswanto 2019).

2.2. Ligands and Receptors Preparation

Preparation of each test ligands was carried out with the YASARA Structure software. Test ligands consisting of compounds 6XO32ZSP1D, Ethyl L-serinate hydrochloride, Schisandrin B, Columbin, compound of N-1,N-9-Bis [E-(2-nitrophenyl) methylene] non anedihydrazide, compound 4-(4-methoxy-phenylamino)-2,3-dihydro-1H-4a, 9-diaza-cyclopenta (b) fluorine-10-carbonitrile, also compound of 6-Amino-4-[3-(belzyloxy) phenyl]- 3- tert -butyl- 2,4- dihydropyrano[2,3-c] pyrazole-5-carbonotrile, and lastly, compound 4-({4,6-Bis[(3R,5S)-3,5-diamino-1-piperydinyl]-1,3,5-triazin-2-yl}amino)benzenesulfonamide in SDF format with three-dimensional form obtained from the PubChem Compound database. The 8 ligands used here are based on reserach by Wedaswari (2018). The geometry of the test ligands was optimized with energy minimization technique to form a more stable and optimal molecular conformation.

The next step was receptors preparation with YASARA Structure software. The receptors used were target proteins from 3D modeling results of human Leukotriene A4 hydrolase, Chek1, and Bcl 2 navitoclax analog. Unneeded parts in the docking protocol were removed, such as water molecules, residues, and native ligands. After that, hydrogen atoms were added while aliphatic hydrogens were not displayed (Agistia *et al.* 2013).

2.3. Molecular Docking Validation

Validation of molecular docking is carried out by directed molecular docking using YASARA Structure by the targeted docking method. The ligand docking zone was bounded by a gridbox around the active side on all three 3D proteins. Gridbox validation began with the stage of re-docking the natural ligands of the preparation results as well as receptors were being re-docked 999 times by YASARA Structure. The gridbox validation was then continued by determining the best gridbox size, also to obtain the RMSD (root mean square distance) value. The gridbox with the best size which had RMSD score less than 2 was then selected so that it can be used in molecular docking simulations (Agistia *et al.* 2013). The gridbox size tested was from size 0, 0.5, 1.0, 1.5 to size 5 with YASARA structure.

2.4. Physicochemical Predictions of Ligands

Lipinski's prediction of test ligands should be done first before molecular docking simulation. The physicochemical properties were tested on Lipinski SCFBio website (http:/Avww.scfbioiitd.res.in/software/dr ugdesign/lipinski.jsp) which is based on the five rules of Lipinski (Adriani 2018). There should not be more than two rules violation in this step.

2.5. Molecular Docking Simulation

Molecular docking of test ligand was carried out with the optimum gridbox size obtained from the

previous gridbox validation. The receptor preparation file was opened in yasara structure software. The file was then prepared by forming a ligand-receptor complex based on the optimum gridbox. The docking results that have been obtained were then read with notepad software. Docking results such as binding energy values and non-covalent interactions of ligand-receptor complexes were obtained from this step (Agistia *et al.* 2013).

2.6. Data Analysis

Molecular docking results were analyzed by looking at the value of the Gibbs free energy (ΔG*/ binding affinity), the inhibition constant (Ki) and the interaction of amino acid residues. The value of Gibbs free energy was used in the analysis of the affinity that occurs between the ligand and the receptor, further analysis of the results of molecular docking 3D visualization of the complex formed between the test ligand and the receptor. The visualization consisting of analysis of hydrogen, hydrophobic interactions, and distances performed with Discovery Studio software.

3. Results

3.1. Protein Structure Quality

The results of the protein structure stability quality of 4LXD receptor with a crystallography resolution of 1.90 Å showed that the protein was the most stable, where as many as 121 residues (96.0%) were in the most favored region and as many as 5 residues (4.0%) in additional allowed region (Figure 1). Followed by 3U9W receptor that got 501 residues in total (92.4%) in the most favored region and 39 residues (7.2%) in additional allowed region (Figure 1), in addition to which this receptor has a crystallography resolution of 1.25 Å. The last resptor tested for stability was 2R0U with 1.90 Å resolution, at this receptor there were 204 residues (87.6%) in the most favored region,

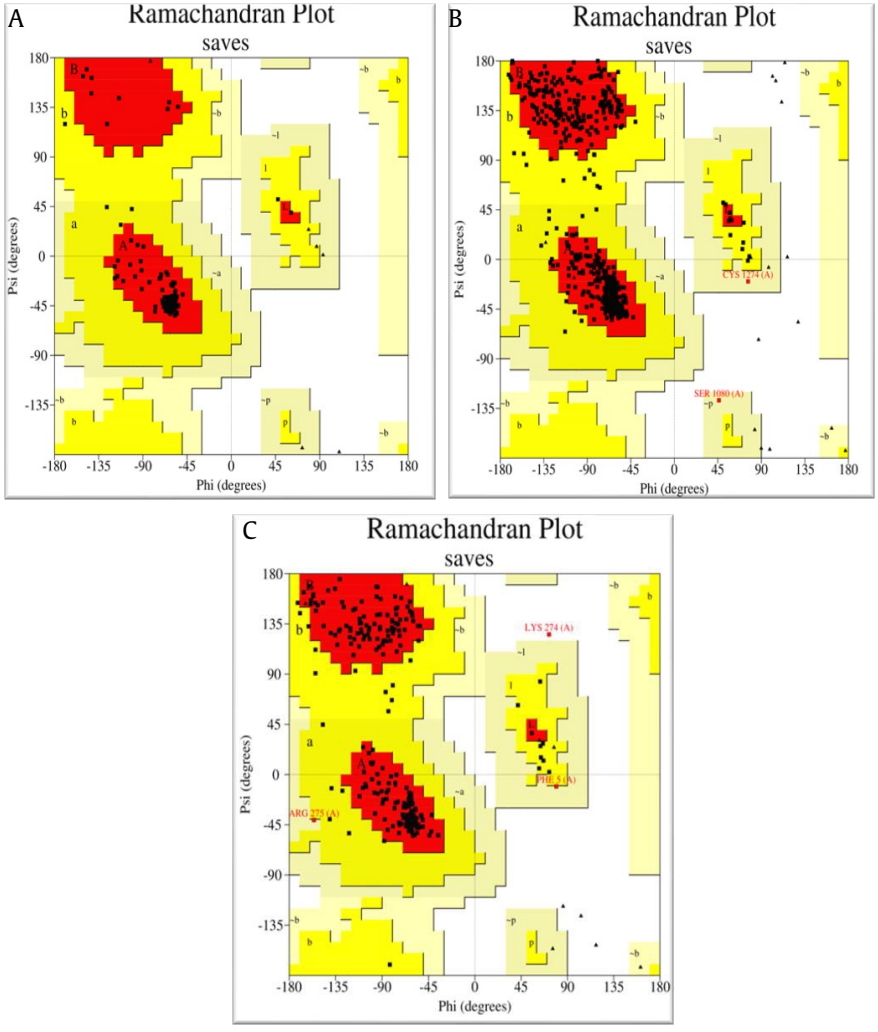

Figure 1. Ramachandran plot of protein. (A) Bcl 2 navitoclax analog (PDB: 4LXD), (B) human Leukotriene A4 hydrolase (PDB: 3U9W), (C) Chek1 (PDB: 2R0U)

and as many as 26 residues (11.2%) were in additional allowed region (Table 1).

3.2. Molecular Docking Validation

The result of the molecular docking validation of each receptor showed that the 4LXD receptor best RMSD score was found at a gridbox size of 3 Å with 3D visualization shown in Figure 2, with an RMSD score of 1.6731 Å, the best binding affinity energy obtained was 6.3880 Kcal/mol. The 3U9W receptor got the best RMSD score of 0.0664 Å at a gridbox size of 3.5 Å with a binding affinity energy of 13.4720 Kcal/mol, and the 2R0U receptor had the best RMSD score which was 0.6895 Å at gridbox with a size of 4 Å, also with a binding affinity energy of 8.1350 Kcal/mol. These gridbox optimum size, binding affinity enrgy score, dissociation constant, and RMSD score of each receptor can be seen in Table 2.

Table 1. Crystallography resolutions and Ramachandrand plot results of receptors

PDB code	Crystallography resolution (Å)	Most favored region (%)	Additional allowed region (%)	Generously allowed (%)	Disallowed region (%)
4LXD	1.90 Å	96.0	4.0	0.0	0.0
3U9W	1.25 Å	92.4	7.25	0.4	0.0
2R0U	1.90 Å	87.6	11.2	0.9	0.4

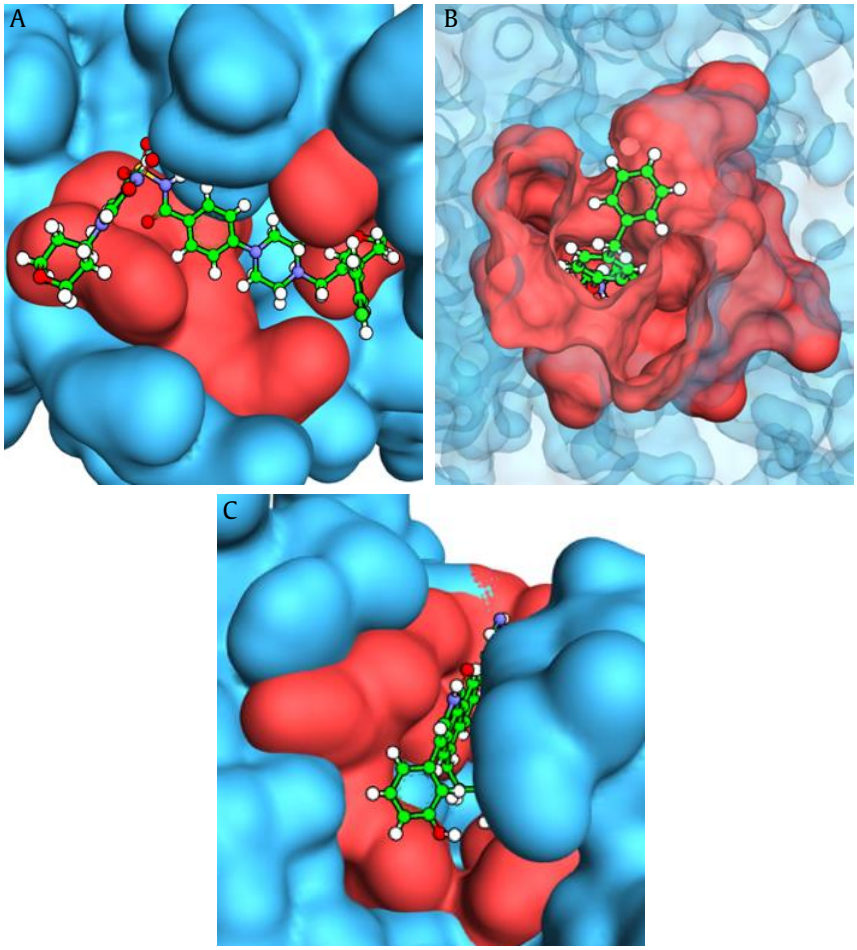

Figure 2. Validation 3D visualization. (A) Bcl 2 navitoclax analog (PDB: 4LXD), (B) human Leukotriene A4 hydrolase (PDB: 3U9W), (C) Chek1 (PDB: 2R0U)

Table 2. Gridbox validations of receptors

PDB code	Gridbox (Å)	Binding affinity energy (Kcal/mol)	Dissoc Constant (pM)	RMSD (Å)
4LXD	3.0	6.3880	20774660	1.6731
3U9W	3.5	13.4720	133.3193	0.0664
2R0U	4.0	8.1350	1088844.6250	0.6895

3.3. Physicochemical Predictions of Ligands

Analysis with the Lipinski Rule of Five of eight test ligands of compounds isolated from the ethyl acetate fraction of red betel leaves passed all test ligands used. Even though ligand with CID code of 2724185 has one violation with molar refractivity rule that has score less than 40 (Table 3) and ligand 44418672 has two violations with hydrogen donor more than 5 bounds, and the hydrogen acceptor more than 10 bounds.

The remaining ligands passed this stage without any rule breakage at all. Specifically in this selection step the ligand is still acceptable if it did not break more than two rules. Therefore these two ligands are still acceptable for next analysis.

3.4. Ligand Docking to BCL 2 Navitoclax Analog Receptor

The interactions that occurred at the Bcl 2 navitoclax analog receptor (PDB: 4LXD) resulted in the best binding affinity energy, which was 8.4470 Kcal/mol with a compound of 4-(4-methoxy-phenylamino) -2.3- dihydro-1H-4a,9- diaza-cyclopenta (b)fluorine-10-carbon itrile with CID number 1077234, shown by Figure 3 with a value of Ki 6.33 x 10^{-7} µM. The results from Table 4 show that there are 12 residues involved in the interaction of ligand and this receptor, of which 7 residues are active site residues, namely Tyr105, Met112, Glu133, Leu134, Gly142, Arg143, and Ala146. There were no hydrogen bonds from ligand and receptor, but there were hydrophobic interactions with 7 residues (Table 5).

3.5. Ligand Docking to Human Leukotriene A4 Hydrolase Receptor

Molecular docking on Human Leukotriene A4 Hydrolase receptor (PDB: 3U9W) showed the best interaction with compound N-1,N-9-Bis [E-(2-nitrophenyl) methylene] non anedihydrazide (CID: 9595915) with a binding affinity energy of 11.3160 Kcal/mol, the best Ki (Inhibition constant) value of

Table 3. Test ligands characteristics based on Lipinski Rule of Five

CID	Molecular weight (Da)	Hydrogen donor	Hydrogen acceptor	LogP	Molar refractivity
75019	210.0	1	4	1.7210	55.502789
108130	400.0	0	6	4.4875	109.944969
188289	358.0	1	6	2.5327	88.555771
1077234	354.0	1	4	4.6000	105.714684
2724185	169.5	3	3	1.2721	39.672199
9595915	482.0	2	6	1.7892	115.112801
44418672	477.0	11	13	-0.9271	126.530701
286545476	258.0	0	3	-2.9124	48.790504

Table 4. Molecular docking of the best ligand with each receptor

PDB code	CID	Binding affinity energy (Kcal/mol)	Inhibition constant (µM)	Amino acid residues
4LXD	1077234	8.4470	6.33 x 10^{-7}	Phe101, Tyr105, Asp108, Phe109, Glu111, Met112, Glu133, Leu134, Gly142, Arg143, Ala146, Phe150
3U9W	9595915	11.3160	4.97 x 10^{-9}	Gln1134, Gln1136, Ala1137, Tyr1267, Gly1268, Gly1269, Met1270, Asn1291, Val1292, His1295, Glu1296, Trp1311, Asp1312, Phe1314, Trp1315, Leu1365, Val1366, Val1367, Leu1369, Pro1374, Asp1375, Ala1377, Tyr1378, Ser1379, Pro1382, Tyr1383, Arg1563, Lys1565
2R0U	44418672	9.7110	7.48 x 10^{-8}	Leu15, Gly16, Val23, Ala36, Lys38, Glu55, Val68, Leu84, Glu85, Tyr86, Cys87, Ser88, Gly90, Glu91, Lys132, Glu134, Asn135, Leu137, Ser147, Asp148, Phe149

4.97 x 10^{-9} µM shown in Table 4. Software analysis showed that the ligand interacted with 28 residues in total, 14 of which are receptor active site residues consisting of Gln1136, Tyr1267, Gly1269, Met1270, His1295, Glu1296, Trp131, Phe1314, Val1367, Pro1374, Ala1377, Tyr1378, Pro1382, and Tyr1383. The interactions of hydrogen bond were found with the Gly1268, Arg1563, and Tyr1383 residues. There were also hydrophobic interactions occurred between the ligand and 18 residues from the 3U9W receptor shown in Table 5. The 3D visualization of this protein and ligand interaction shows that the catalytic area is wide enough to cover ligand's surface, and wider than 4LXD and 2R0U receptor, this is due to the large number of residues involved in molecular docking (Figure 3).

3.6. Ligand Docking to Chek1 Receptor

The Chek1 receptor (PDB: 2R0U) showed the best interaction result with a ligand compound of 4-({4,6-Bis[(3R,5S)-3.5-diamino-1-piperydinyl]-1,3,5-triazin-2-yl}amino) benzenesulfonamide (CID: 44418672) with visualization result shown in Figure 3. The binding affinity energy between this ligand and the 2R0U receptor was 9.7110 Kcal/mol, with a value of Ki 7.48 x 10^{-8} µM, and interacted with 21 residues, and 12 of them are active site residues, namely Leu15, Val23, Lys38, Leu84, Tyr86, Cys87, Ser88, Gly90, Glu91, Glu134, Asn135, and Leu1237 (Table 4). The hydrogen bond interactions were found in the Asp148 and Glu91 residues, besides that it also has hydrophobic interactions with 9 residues from the receptor (Table 5).

Table 5. Interaction of the best ligand amino acids with each receptor

PDB code	CID	H-bound residue	H-bound length (Å)	Atom interaction	Hydrophobic interaction
4LXD	1077234	-	-	-	Tyr105, Ala146, Leu134, Glu133, Asp108, Met112, Phe101
		Gly1268	3.17	Oxygen	Lys1565, Gly1269, Glu1296,
		Arg1563	3.05	Oxygen	Tyr1267, Gln1136, Asp1375,
3U9W	9595915		2.98	Oxygen	Ala1137, Ala1377, Leu1368,
		Tyr1383	2.91	Oxygen	Asp1312, Trp1311, Val1367, Leu1365, Pro1382, Phe1314, Tyr1378, Pro1374, Val1292
2R0U	44418672	Asp148	3.02	Nitrogen	Ser147, Glu134, Leu15, Tyr86,
		Glu91	3.01	Nitrogen	Cys87, Leu137, Val23, Leu84, Ala36

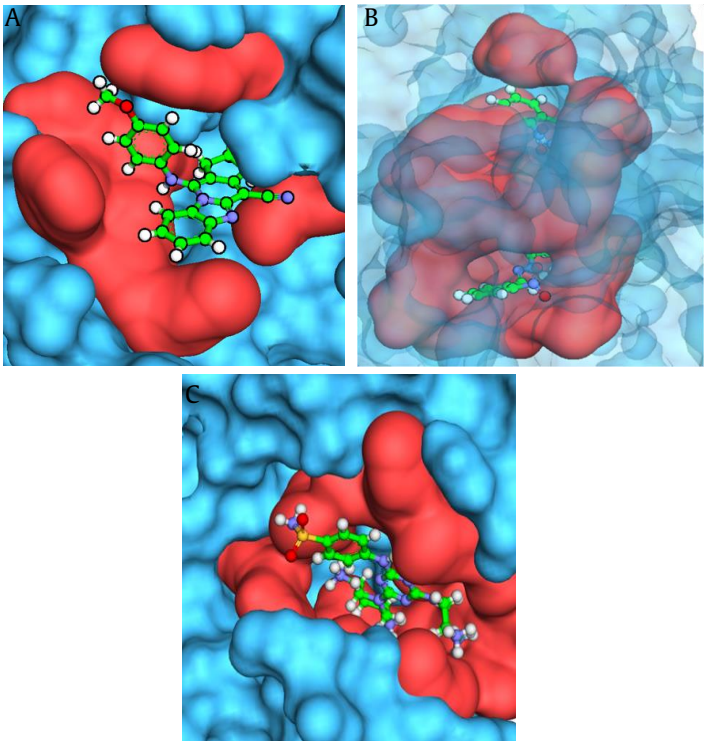

Figure 3. The 3D docking visualization of receptor and its best ligand. (A) Bcl 2 navitoclax analog (PDB: 4LXD), (B) human Leukotriene A4 hydrolase (PDB: 3U9W), (C) Chek1 (PDB: 2R0U)

4. Discussion

4.1. Protein Structure Quality

Diffraction resolution chategory is divided into four categories namely: small (<3.00 Å), medium (2.70-2.00 Å), high (2.00-1.50 Å), and very high (< 1.5 Å). The smaller the crystallographic value, the more specific to image generated visualization (Made and Pathni 2018). this statement indicates that all three receptors used from Figure 1 have high resolution. In addition, the results of the Ramachandran diagram of a structure with >90% residue in favoured regions indicate an accurate structure (Rai and Rieder 2012), it is hereby known that all three receptors also have accurate structure to proceed at the molecular docking stage.

4.2. Molecular Docking Validation

The validation stage aims to ensure that the size of the grid box obtained is appropriate and already includes the active side of the tested receptor. The validation stage will produce an RMSD value that will show the accuracy of the docking conformation that has been carried out. Docking results are considered good if it has an RMSD value of less than 2 Å (Purnomo 2013). Therefore, from this statement, it is concluded that the three receptors are accurate and good for use in the molecular docking stage (Table 2) while the 3D visualization results of the validation of each receptor are shown in Figure 2.

4.3. Physicochemical Predictions of Ligands

Lipinski's rules are used to evaluate the drug likeness of a chemical compound. The rules consist of a molecular weight of <500 Da, a LogP value of <5, the number of hydrogen bond donors <5, the number of acceptors of hidrogen bond <10 and a molar refractivity between 40-130 (Dwi and Abdul 2011). Results from Table 3 shows that all eight test ligands have very high bioavailability because the highest violations are only two rules. Thus it can be concluded that the compounds have good compatibility because they pass these rules and shows that these compounds have the potential to have similarities in orally active drugs (Tumilaar *et al.* 2021). In addition, these things indicate that each of the compounds easily binds to receptors and how well the permeability of the compounds are in crossing the cell membrane (Singh *et al.* 2013).

4.4. Ligand Docking to BCL 2 Navitoclax Analog Receptor

Previous reasearch showed that in XP docking kaempferitrin with BCl-2 (PDBID: 4LXD), there were five interactions of hydrogen bond with essential amino acids Asp100 (bond length, 2,050 Å), Tyr199 (bond length, 2,647 Å), Asn140 (bond length, 2,281 Å), Arg143 (bond length, 2,033 Å), Asp108 (bond length, 2,136 Å) (Govindarasu *et al.* 2021). Based from the results of this study, these residues were found to be involved in the docking of receptors and red betel leaves test compounds.

4.5. Ligand Docking to Human Leukotriene A4 Hydrolase Receptor

The results of 3D visualization between the receptor and the ligand that have the best binding affinity energy are shown by Figure 3. The Parameters observed for the determination of the energy of the ligand affinity to the receptor in this study ware the binding affinity energy, the value of the inhibition constant, and the amino acid residue. When hydrophobic bonds increase from a drug compound, the activeness of the compound will increase (Patil *et al.* 2010). The statement corresponds to the 3U9W receptor where as the hydrophobic bond increases, the better the affinity score, and the smaller the value of Ki or its inhibition constant. The value is the concentration of inhibitors needed to decrease by half the activity of the enzyme. The smaller the value of Ki, the stronger the inhibitor (Pannindriya *et al.* 2021).

Previous studies have shown that active pocket located in the area of the N-terminal catalytic domain which is hydrophobic. The docking results showed that the interaction of short length bonds and the number of hydrogen bonds formed was found more in the interaction of protein Leukotriene A4 Hydrolase-Bullatalisin than the protein Leukotriene A4 Hydrolase-standard, the compound bullatasin itself is an acetogenin derivative compound that has the potential to become an inhibitor against Leukotriene A4 hydrolase. Bullatalicin ligands, along with standard ligands can occupy protein active pocket alternative of leukotriene A4 Hydrolase receptors (Noviardi and Fachrurrazie 2015).

3.6 Ligand Docking to Chek1 Receptor

The Chek1 protein is necessary for effective cell division in the phases of the normal cell cycle, so that both during cancer development and progression and under stressful environments, the amount of Chek1 protein is strictly controlled (Zhang and Hunter 2013). These findings suggest that inhibiting Chek1 can be an effective treatment for cancers that overexpress the protein. The study on kaempferitrin docking with Serine/threonine-protein kinase Chek1 (PDBID: 2R0U), showed 8

correlations of hydrogen bonds with vital amino acids Ser88 (bond length, 2,054 Å), Tyr86 (length, 2,037 Å), Asp94 (bond length, 2,106 Å), Cys87 (bond length, 2,233 Å), Glu85 (bond length, 2,526 Å), Asp148 (bond length, 2,505 Å), Glu55 (length, 1.84 bond4 Å), Lys38 (bond length, 2,293 Å) (Govindarasu *et al.* 2021). Based on the results of previous studies, some of these residues are broadly involved in the interaction with red betel leaves test ligands, including with test ligand that interacted best with it.

The conformation of docking is determined from the result of the highest affinity in the form of bond energy (ΔG) with YASARA structure. Analysis of molecular interactions can show specific interactions between ligands and receptors. The interactions between ligands and receptors are stabilized by hydrogen bonds and hydrophobic reactions (Perdana and Permana 2021). The binding affinity energy score will affect the intermolecular activity of the compound and have an impact on the strength of the bond. The best binding affinity energy score will provide greater strength of protein and ligand interaction (Hanif *et al.* 2020), therefore the 3U9W and 2R0U receptors interact most strongly with the ligands with the best binding affinity energy.

In conclusion of this research there are several compounds that have the potential as inhibitors against colon cancer marker proteins by *in silico* method to inhibit the development of colorectal cancer and have high bioavalibility as oral drugs. The compound N-1,N-9-Bis [E-(2-nitophenyl) methylene] non anedihydrazide has the highest inhibition of human leukotriene A4 hydrolase. The next compound is 4-({4,6-Bis[3R,5S)-3,5-diamino-1-piperydinyl]-1,3,5-traizin-2-yl} amino) benzenosulfonamide which has the highest inhibition in Chek1 and the compound 4-(4-methoxy-phenylamino)-2,3-dihydro-1H-4a, 9-diaza-cyclopenta (b) fluorine-10-carbonitrile has the highest inhibition in the Bcl 2 navitoclax analog receptor.

Acknowledgements

The writer of this article would like to thank Indonesia Collaborative Research–WCU (World Class University) fiscal year of 2020 Number: 1755/IT3.L1 PN/2020/IT3.L1/PN/2020 on the behalf of Dr. Mega Safithri, S.Si., M.Si. who helped fund this article.

References

Adriani, 2018. Prediction of bioactive compounds from sanrego plant (*Lunasia amara* Blanco) as inhibitors of the enzyme cyclooxygenase-2 (COX-2) through molecular docking. *JIP*. 1, 6-11.

Agistia, D.D., Purnomo, H., Tegar, M., Nugroho, A.E., 2013. Interaction between active compounds from Aegle marmelos Correa as anti inflammation agent with Cox-1 and Cox-2 receptor. *Traditional Medicine Jurnal*. 18, 80-87.

Dwi, H., Abdul, K., 2011. *Pengantar Kimia Komputasi.* Lubung Gung Press, Bandung.

Florea, A., Busselber D., 2011. Cisplatin as an antitumor drug: cellular mechanism of activity, drug resistance and induced side effect. *Cancer (Basel)*. 3, 1351-1371. https://doi.org/10.3390/cancers3011351

Govindarasu, M., Ganeshan, S., Ansari, M.A., Alomary, M.N., AlYahya, S., Alhamdi, S., Almehmadi, M., Rajakumar, G., Thiruvengadam, M., Vaiyaputri, M., 2021. *In silico* modeling and molecular docking insights of kaempferitrin for colon cancer-related molecular targets. *Journal of Saudi Chemical Society*. 2021, 1-21. https://doi.org/10.1016/J.JSCS.2021.101319

Hanif, A.U., Lukis, P.A., Fadlan, A., 2020. Pengaruh minimisasi energi MMFF94 dengan MarvinSketch dan open babel PyRx pada penambatan molekular turunan oksindola tersubstitusi. *Alchemy : Journal Of Chemistry*. 8, 33-40. https://doi.org/10.18860/al.v8i2.10481

Kurnia, S.N., Ruswanto, 2019. Studi komputasi senyawa 1,3-bis (methylsulfinyl) benzene dengan metode simulasi dinamika molekuler pada aplikasi gromacs 2019. *In: Prosiding Seminar Nasional dan Penelitian Kesehatan 2018, Tasikmalaya 2018*. Tasikmalaya: Semnaskes. pp. 1-5.

Made, P., Pathni S.D., 2018. Trend in diabetes therapy with GLP-1 receptor agonists. *CDKJournal*. 45, 291-296. https://doi.org/10.1007/978-3-319-27317-4_20-1

Noviardi, H., Fachrurrazie., 2015. The potency of bullatalicin as an inhibitor of Leukotrienea4 Hydrolase protein in colon cancer by *in silico* study. *Fitofarmaka.* 5, 65-73. https://doi.org/ 10.33751/jf.v5i2.410

Pannindriya, P., Safithri, M., Tarman, K., 2021. *In silico* analysis of spirulina platensis active compounds as tyrosinase inhibitor. *JPHPI*. 24, 70-77. https://doi.org/10.17844/jphpi.v24i1.33122

Patil, R., Das, S., Stanley, A., Yadaf, L., Sudhakar, A., Varma, A.K., 2010. Optimized hydrophobic interactions and hydrogen bonding at the target-ligand interface leads the pathways of drug designing. *PloS ONE*. 5, 1-10. https://doi.org/10.1371/journal.pone.0012029

Perdana, A.T., Permana, A.A., 2021. Molecular docking senyawa potensial anticovid-19 secara *in silico. JIKA*. 5, 159-166. https://doi.org/10.31000/jika.v5i2.4516

Purnomo, H., 2013. *Kimia Komputasi: Molecular Docking Plants [Protein-ligand-antsystem] ("Ilmu Semut").* Pustaka Pelajar, Yogyakarta.

Putri, W.S., Warditiani, N.K., Larasanty, L.P.F., 2013. Skrining fitokimia ekstrak etil asetat kulit buah manggis (*Garcinia mangostana* L.). *Jurnal Farmasi Udayana*, 2, 56-60.

Rai, D.K., Rieder, E. 2012. Homology modeling and analysis of structure predictions of the bovine rhinitis B virus RNA dependent RNA polymerase (RdRp). *International Journal of Molecular Sciences*. 13, 8998-9013. https://doi.org/10.3390/ijms13078998

Rizki, K., Hal, Rochmah, W.W.W., Cempaka, N.G., Hartono, S., Fajrin, F.A., 2015. Anticancer activity of cacao pod husk pectin toward amount of colon goblet cells. *Indonesian Journal of Pharmaceutical Science and Technology*, 2, 75-82. https://doi.org/10.15416/ijpst.v2i3.7903

Rosyadi, A., Faizah, R.N., Nuri, N., Puspitasari, E., 2020. Anticancer properties of methanolic extract of *Piper crocatum* leaf using BST and cytotoxicity on HeLa cell lines. *Annals of Tropical Medicine and Public Health*. 23,1-9. https://doi.org/10.36295/ASRO.2020.2331

Safithri, M., 2012. Study on Antihyperglycemic Mechanism of Extract Mixture of *Piper crocatum* Leaves and *Cinnamomum burmannii* Bark as Potential Functional Drink [Dissertation]. Bogor, Indonesia: Bogor Agricultural University.

Safithri, M., Suminto, S., Kurniawati, A. 2016. Formula of *Piper crocatum, Cinnamomum burmanii*, and *Zingiber officinale* extracts as a functional beverage for diabetics. *International Food Research Journal*, 23, 1123-1130.

Sayuti, M., Nouva., 2019. Colorectal cancer. *Averrous*. 5, 76-88. https://doi.org/10.29103/averrous.v5i2.2082

Singh, S., Gupta, A., Verma, A., 2013. Molecular properties and bioactivity score of the aloe vera antioxidant compounds in order to lead fnding. *Research Journal of Pharmaceutical, Biological and Chemical Sciences*. 4,876–881.

Suyanto, E., Momuat, L.I., 2017. Isolation and antioxidant activity of the fractions of corncob (Zea mays) extract. Agritech, 37, 139-147. https://doi.org/10.22146/agritech.27537

Tumilaar, S.G., Siampa, J.P., Tallei, T.E., 2021. Molecular docking of bioactive compounds from pangi (*Pangium edule*) leaves ethanol extract against HIV-1 protease. *Jurnal Ilmiah Sains*. 21, 6-16. https://doi.org/10.35799/jis.21.1.2021.30282

Wedaswari, I.A.I., 2018. Activity of Ethanol Extract and Fractions of *Piper crocatum* with Rancimat Method and Identify with LC-MS [Thesis]. Bogor, Indonesia: Bogor Agricultural University.

Wicaksono, B.D., Handoko, Y.A., Arung, E.T., Kusuma, I.W., Yulia, D., Pancaputra, A.N., Sandra, F., 2009. Antiproliferative effect of the methanol extract of *Piper crocatum* Ruiz and Pav leaves on human breast (T47D) cells *in-vitro*. *Tropical Journal of Pharmaceutical Research*, 8. 345-352. https://doi. org/10.4314/tjpr.v8i4.45229

Zhang, Y., Hunter, T., 2013. Roles of Chk1 in cell biology and cancer therapy. *Int. J. Cancer*. 134, 1013–1023. https://doi. org/10.1002/ijc.28226